

https://doi.org/10.1070/QEL17659

Optical fibres with an inscribed fibre Bragg grating array for sensor systems and random lasers

S.M. Popov, O.V. Butov, A.O. Kolosovskii, V.V. Voloshin, I.L. Vorob'ev, V.A. Isaev, D.V. Ryakhovskii, M.Yu. Vyatkin, A.A. Rybaltovskii, A.A. Fotiadi, Li Xia, Zhuoying Wang, D.S. Lipatov, Yu.K. Chamorovsky

Abstract. **We report the latest results on inscribing extended fibre Bragg grating (FBG) arrays upon fibre drawing, obtained at the Kotelnikov Institute of Radioengineering and Electronics of RAS. The properties of these structures are considered, and examples of their application in sensor systems of microwave dense wavelength multiplexing and as a basis for designing single-frequency fibre lasers are considered. The optical and laser characteristics of FBG arrays, inscribed (using 248-nm UV laser radiation) both in standard single-mode telecommunication fibres of the SMF-28 type and in erbium-doped active fibres, are investigated.**

Keywords: *fibre Bragg grating arrays, optical sensors, microwave demodulation, active optical fibres, fibre lasers.*

1. Introduction

Optical fibres (OFs) are widely used both as data transmission lines and in sensor systems. In the latter case, when designing distributed sensor systems, one often needs OFs, whose backward signal significantly exceeds the Rayleigh backscattering level. The importance of designing OFs with enhanced backward signal is related to the active development of some new lines of research in applied photonics: random lasers, coherent reflectometry, and three-dimensional shape sensors [1 – 7].

Fibre Bragg grating (FBG) arrays are generally used to increase the backward signal intensity. These structures are inscribed by UV radiation in several stages: first a polymer coating is removed from an OF segment ~10 mm long; then an FBG is formed in it using UV laser radiation; and, finally, this OF segment with inscribed FBG is coated again with a polymer. Then the entire procedure is repeated on the next OF segment. This approach allows one to increase significantly the backward signal; however, it deteriorates the OF mechanical strength in the regions with inscribed FBGs, thus reducing essentially the FBG array potential and range of application. In addition, the number of FBGs in such an array is limited. The technique of femtosecond inscription by visible or IR laser radiation is free of these drawbacks, because one can do without removing coating in this case [5, 8]. However, both these methods for fabricating large FBG arrays require significant (and often unjustified) efforts.

The problem was solved by developing special OFs with extended FBG arrays inscribed by UV radiation directly during OF drawing [9 – 15]. An FBG is inscribed using UV excimer laser pulses and a phase mask. The number of FBGs per a 100-m segment of this OF may be as high as 10000, and the ratio of the backward signal to the Rayleigh scattering level (contrast) may reach 50 dB at the Bragg wavelength λ_B. A typical width of the reflection spectrum of an extended FBG array inscribed during drawing (at 100% filling by OF gratings) is 0.3 nm. Using a chirped phase mask to inscribe an FBG array, one can obtain arrays with a total reflection spectrum width of 4 nm, which is necessary for their application in coherent reflectometry systems operating in a wide temperature range [15, 16]. However, the level of reflected signal may decrease in this array.

Extended FBG arrays can also be formed in active OFs doped with rare-earth ions. This approach allows one to design OFs possessing both enhanced reflectance and possibility of forming dynamic gratings in them, which are important for spectral selection of laser radiation [17, 18].

As compared with Rayleigh backscattering in conventional OFs, the backscattering in OFs with an inscribed FBG array is characterised by a fairly narrow reflection spectrum; the total spectral width is determined by the width of the reflection spectrum of individual FBGs. However, within a reflection line, the reflection spectra of OFs with an FBG array are similar to Rayleigh scattering spectra. They are characterised by random (Rayleigh) frequency distribution of reflectance amplitude and have a form of alternating maxima and minima on a typical scale, determined by the time of backward light propagation throughout the entire fibre length. Thus, if the working frequency range lies within the grating reflection spectrum, OFs with an FBG array, being a good alternative to conventional Rayleigh fibres, can be efficiently used, in particular, in such applications as coherent reflectometry [15, 16] and random lasers [17, 18].

S.M. Popov, A.O. Kolosovskii, V.V. Voloshin, I.L. Vorob'ev, V.A. Isaev, D.V. Ryakhovskii, M.Yu. Vyatkin, Yu.K. Chamorovsky Kotelnikov Institute of Radioengineering and Electronics (Fryazino Branch), Russian Academy of Sciences, pl. Vvedenskogo 1, 141190 Fryazino, Moscow region, Russia; e-mail: sergei@popov.eu.org;
O.V. Butov, A.A. Rybaltovskii Kotelnikov Institute of Radioengineering and Electronics, Russian Academy of Sciences, ul. Mokhovaya 11, korp. 7, 125009 Moscow, Russia;
A.A. Fotiadi University of Mons, 31 Boulvard Dolez, Mons 7000, Belgium; Ulyanovsk State University, ul. L. Tolstogo 42, Ulyanovsk 432700 Russia;
Li Xia, Zhuoying Wang Huazhong University, 1037 Road LuoYu, Wuhan 430074, China;
D.S. Lipatov G.G. Devyatykh Institute of Chemistry of High-Purity Substances, Russian Academy of Sciences, ul. Tropinina 49, 603950 Nizhny Novgorod, Russia

Received 26 October 2021
Kvantovaya Elektronika **51** (12) 1101 – 1106 (2021)
Translated by Yu.P. Sin'kov

2. Experimental

A schematic of the experimental setup used to inscribe FBG arrays is presented in Fig. 1. The portion of the fibre extension column that precedes the protective coating deposition zone contains an FBG inscription system. An Optosystems CL-5100 pulsed excimer KrF laser [19] with a lasing wavelength 248 nm is used as an UV source. The pulse energy density for each inscribed FBG was 400 mJ cm^{-2} (for a pulse duration of 10 ns). This high density was provided by focusing the laser beam by a cylindrical lens with a focal length $f' =$ 95 mm. A phase mask was installed at a distance of 117 mm from the lens. The optical scheme contained also a diaphragm for controlling the size of the beam transmitted through the mask. We applied an Ibsen Photonics phase mask with a working length of 10 mm and a period $L = 1070$ nm. The OF drawing rate was ~6 m min^{-1}.

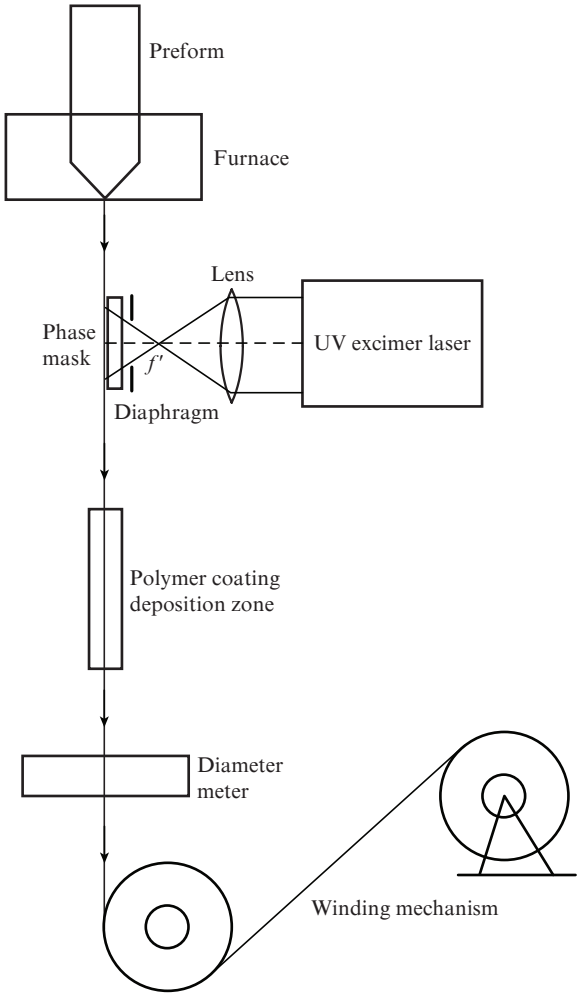

Figure 1. Schematic of the experimental setup for inscribing FBG arrays.

A single FBG is inscribed in an array in each pulse. The phase mask is located in a close proximity of drawn fibre. The typical length of a single FBG, which is determined by the laser-beam width and the phase mask working length, amounts to 10 mm. The on–off time ratio of FBG repetition along the fibre length (inscription density) is controlled by synchronising the drawing rate and the UV-pulse repetition rate. For example, complete (100%) filling of OF with single FBGs was obtained at a pulse repetition rate of 10 Hz and a drawing rate of 6 m min^{-1}. A decrease in the pulse repetition rate to 5 Hz at the same drawing rate results in 50% filling of OF with single FBGs. In this case, the distance between single FBGs is equal to their length: 10 mm. When taper OFs are drawn, the change in their diameter is determined by the change in the OF preform feeding rate.

FBG arrays were inscribed using preforms with a low content of germanium oxide in the core (germanosilicate glass). The waveguide parameters of the fibres drawn from these preforms correspond to the G.652 specification.

An experiment on inscribing an extended FBG array in an active OF was performed using a specially synthesised preform with a germanophosphosilicate glass core doped additionally with erbium ($Er_2O_3/GeO_2/P_2O_5/SiO_2$). At low concentrations of erbium ions the phosphosilicate matrix provides their fairly uniform distribution over the glass network (without the formation of large cluster elements), and the germanium oxide additive increases the core material photosensitivity to UV radiation. The erbium fibre preform was fabricated completely by modified chemical vapour deposition using low-volatile chelate $Er(thd)_3$, thermostated at 157 °C. A thin-wall quartz tube Heraeus (15 × 12.4; F300 grade) was used to produce a preform. First several layers of $F–P_2O_5–SiO_2$ glass of reflecting cladding, with a refractive index somewhat lower than that of quartz glass, were deposited. The next step (after preliminary tube compression to an inner diameter of 5–6 mm) was the core deposition. The deposition of a reflecting cladding and preliminary compression of the support tube made it possible to reduce the evaporative loss of volatile components (P_2O_5 and GeO_2) and make narrower the central hole in the core refractive index profile.

The core glass was synthesised according to an original technique implying separate deposition of its components [20, 21]. First a porous layer of $GeO_2/P_2O_5/SiO_2$ matrix was deposited at a low temperature (1400 °C). Then a mixture of $Er(thd)_3$ vapor and oxygen was fed into the tube, and Er_2O_3 particles formed in the heating zone (1300 °C) were deposited on the matrix layer surface, after which the $Er_2O_3/GeO_2/P_2O_5/SiO_2$ layer was molten (at 1950 °C) into a transparent glass in a CCl_4 atmosphere in order to remove the water formed in the impregnation stage. The core was prepared by depositing five matrix layers, with their subsequent impregnation and alloying each layer. Finally, the tube preform was completely consolidated into a continuous rod at a relatively low temperature (1950 °C). The preform was retightened and jacketed to match the first-mode cutoff wavelength (0.94 μm). The difference between the core and cladding refractive indices in the jacketed preform was 0.009.

A test single-mode fibre with a standard diameter of 125 μm was drawn from the preform. The level of 'gray' optical loss in the test fibre turned out to be ~2 dB km^{-1}, a value suggesting homogeneity of the core glass structure and the absence of transition metal impurities in the glass. The intensities of absorption peaks of Er^{3+} ions in maxima at wavelengths of 980, 1490, and 1535 nm were 1.4, 1.2, and 2.8 dB m^{-1}, respectively. A study of the elemental composition of core glass by an X-ray analyser (JEOL 5910LV) showed the average concentrations of P_2O_5 and GeO_2 to be 6.5 and 2.5 mol %, respectively. The erbium concentration turned out to be below the analyser detection limit (less than 0.1 at. %).

The parameters of prepared FBG-array OFs were measured both by frequency reflectometry [22] using a Luna 4400 instrument and by the spectral method using a Yokogawa AQ6370D optical spectrum analyser, having a maximum optical resolution of 0.02 nm. The radiation source for spectral measurements was either a superluminescent diode with fibre output or a halogen lamp.

3. Results and discussion

3.1. Sensor reflectometry on FBG arrays

One of the novel applications of FBG-array fibres is their use in high-throughput systems of microwave signal demodulation [23–27] for measuring the OF temperature or mechanical tension. Advantages of this method are its high spatial resolution (less than 0.5 m) and small error in determining the OF tension (to 0.0001%) [25]. At the same time, its circuitry implementation is relatively simple in comparison with frequency reflectometers [22], Brillouin optical time-domain analysis (BOTDA) systems [28, 29], and Raman reflectometers [29]. Currently, OFs with individual FBGs in an array fabricated by means of manual successive inscription are used as sensing elements in microwave demodulation systems [25].

To integrate maximally FBG-array OFs into existing communication lines, their geometric parameters must coincide with those of standard single-mode fibres (of the SMF-28 type). Deviation of parameters from standard values may lead to undesirable losses at OF splices, which is especially important for reflectometric sensor systems, because both the transmitted and scattered signals are attenuated in this case. For example, when using an FBG array inscribed in a photosensitive OF [11] with a core diameter of 6 μm, its splicing with a standard single-mode SMF-28 OF (core diameter 9 μm) leads to signal attenuation by ~50% and ~75% for single and double passes, respectively. Such a high signal loss is unacceptable for practical applications of these OFs and limits the operating potential of microwave demodulation systems.

Figure 2 shows a frequency reflectogram of an FBG array inscribed upon drawing using a preform for fabricating SMF-28 OFs according to the schematic presented in Fig. 1. The filling density of the FBG array is 100% (100 FBGs per 1-m-long OF segment). The inscription contrast reaches 50 dB at a wavelength of 1548.2 nm, which is 20–25 dB higher

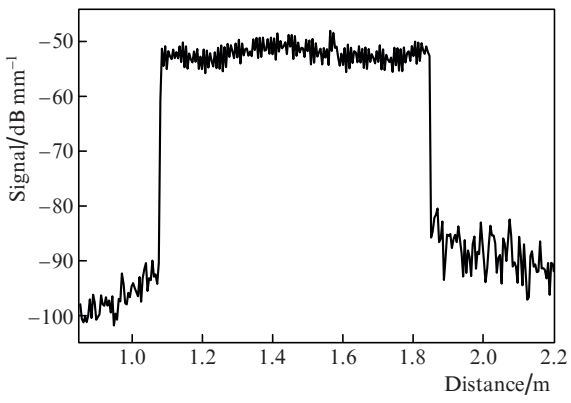

Figure 2. Frequency reflectogram of an FBG array inscribed upon drawing a single-mode SMF-28 OF.

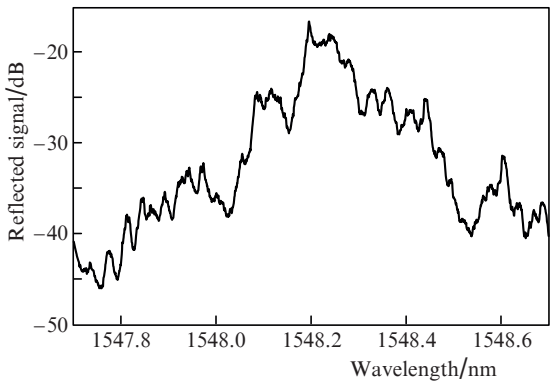

Figure 3. Reflection spectrum of an FBG array inscribed upon drawing a single-mode OF (OF segment length is 1 m).

than the previously obtained inscription contrast for OFs this type [15]. The reflection spectrum is shown in Fig. 3; its width does not exceed 0.4 nm.

The samples obtained are characterised by a high reflectance: up to 15% for a 10-m-long sample. The level of reflected signal for an FBG array is more than sufficient for use in distributed monitoring systems, because strong local reflection leads to fast attenuation of the signal propagating further through the OF and significant diminishing of the monitoring zone.

Figure 4 presents an optical schematic of the experimental setup for microwave signal demodulation [25]. The broadband radiation was provided by an amplified spontaneous emission (ASE) source operating in the C-wavelength range. A polarisation controller (PC) was applied to maintain the radiation polarisation inside the electro-optic modulator (EOM), having a transmission band of 2.5 GHz at a level of 3 dB. An optical circulator (C) was used to input/output radiation into/from an FBG-array OF. A signal was selected by a Finisar WS-AA-4000S-ZZ-H programmable bandpass filter (BPF) and detected by a Newport 1647 photodetector (PD) with a transmission band of 1.1 GHz. Microwave signal spectra were recorded using a Rohde&Schwarz ZVL6 vector network analyser (VNA) with a transmission band of 6 GHz. A 6-m-long FBG-array OF was used in the experiment.

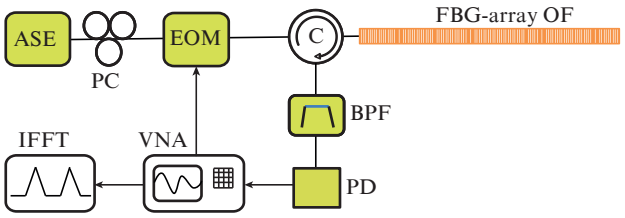

Figure 4. Optical schematic of the experimental setup of microwave signal demodulation.

When the system of microwave signal demodulation operates, an FBG-array OF is exposed to the broadband radiation source. The radiation frequency is additionally scanned in a range up to 2.5 GHz using an EOM. The signal reflected from the FBG array is selected using the BPF and fixed for each frequency (within the EOM scan band) by the photodetector

PD. Demodulation (transformation) of the microwave signal spectrum into a spatial distribution (reflectogram) is performed using inverse fast Fourier transform (IFFT). The impact (e.g., heating or extension) magnitude is determined by subtracting the microwave spectra measured before and after impacting the FBG-array OF.

To carry out an experiment, an FBG-array OF was preliminary fixed on a metal band about 1 m long. The band central part was elevated at a height of 10 cm, which led to bending of the band and extension of the FBG-array OF fixed on it. The OF was extended at two points as a result of its twofold drawing over the metal band (from left to right and vice versa). Figure 5 shows a reflectogram obtained by microwave demodulation, which contains two identical peaks spaced by a distance of about 1.5 m, which correspond to two extension portions of FBG-array OF.

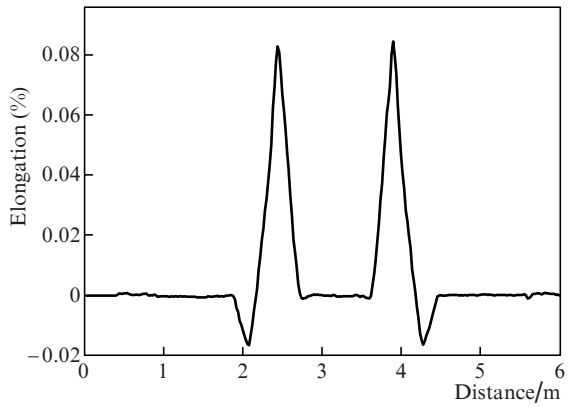

Figure 5. Spatial profile of FBG-array OF extension (microwave demodulation technique).

3.2. FBG arrays with an expanded reflection spectrum

While carrying out the study, further ways to expand the FBG array reflection spectrum were sought for, because there must be reliable correspondence between the coherent-reflectometer source wavelength and the FBG-array reflection wavelength. Obviously, when fabricating and packing a fibre cable, additional stresses may arise, which would change the reflection wavelength of individual FBGs or the entire array. In addition, an expansion of the FBG reflection spectrum will make it possible to increase both the range of measured strains and the working temperature range of sensor systems, because a change in ambient temperature by 1 °C causes shifts of the wavelength (by 10 to 17 pm, depending on the fibre type), the Bragg wavelength, and the temperature range [30, 31]. It was noted previously that, using a chirped phase mask, one can obtain an FBG-array OF with a reflection spectrum as wide as 4 nm [15, 16]. However, a chirped phase mask is not always available for one-shot inscription of an FBG-array OF.

To expand the FBG-array reflection spectrum, the initial standard (with a constant period of 1070 nm) phase mask width of 10 mm was reduced to 1.5 mm using a diaphragm. The diaphragm was located as close as possible to the phase mask. This made it possible to increase the width of FBG-array reflection spectrum to 0.8 nm (Fig. 6) against 0.2 nm, obtained with a phase mask 10 mm wide. The reflected signal level decreased by 4–6 dB in comparison with the signal obtained as a result of FBG inscription by a phase mask without orificing (compare Figs 6 and 3). An expansion of reflected signal spectrum to 0.8 nm makes it possible, in particular, to increase the working temperature range of FBG-array OFs to approximately 70 °C and, correspondingly, expand significantly the range of application of these fibres.

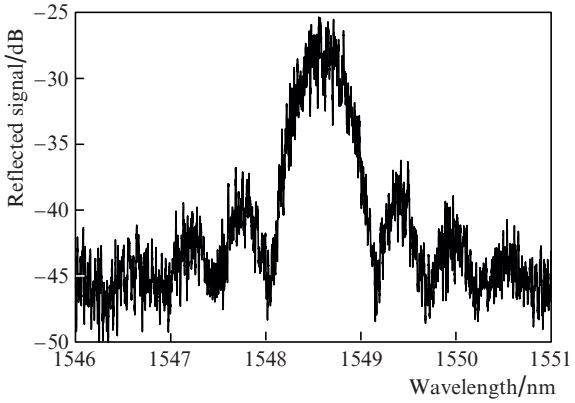

Figure 6. Reflection spectrum of an FBG array inscribed upon drawing a single-mode OF (OF segment length 1 m) using a 1.5-mm-wide phase mask, obtained with the aid of a diaphragm.

3.3. Random lasers based on FBG arrays

One of new applications of FBG arrays is their use as random laser cavities [32–35]. An exposure of a drawn OF to a focused beam of a pulsed UV excimer laser may provide an acceptable contrast level for individual FBGs; therefore, extended FBG arrays can be formed not only in photosensitive fibres with a germanosilicate glass core but also in OFs with low initial photosensitivity, for example, in active OFs with an aluminosilicate glass core, doped additionally with rare-earth ions [17, 18]. However, our recent experiments showed that the contrast of FBGs inscribed upon drawing active OFs with a GeO_2 additive in the core is as minimum an order of magnitude higher than for the active OFs with an aluminosilicate core; this circumstance makes it possible to increase significantly the Q factor of the random laser cavity [36].

In our experiment, two OF samples with FBG inscription densities of 50 and 100% (samples 1 and 2, respectively) were drawn from a preform with a germanophosphosilicate glass core, doped additionally with erbium ions. Figure 7 shows a reflectogram of sample 1. Here, the FBG inscription contrast reached 50 dB at a wavelength of 1547.5 nm. The reflection spectrum of FBG array for a 1-m-long segment of sample 1 is presented in Fig. 8.

The lasing characteristics of sample 2 with a length of ~50 m were investigated in the counter-pumping scheme, which was considered in detail in [15, 17]. Pumping at a wavelength of 1490 nm was performed by an Alcatel A1948FBG diode laser. The emission spectrum of a fibre laser based on sample 2 is presented in Fig. 9. The laser intensity peak (1547.55 nm) coincides with the maximum of FBG array reflection. The maximum output power of the investigated

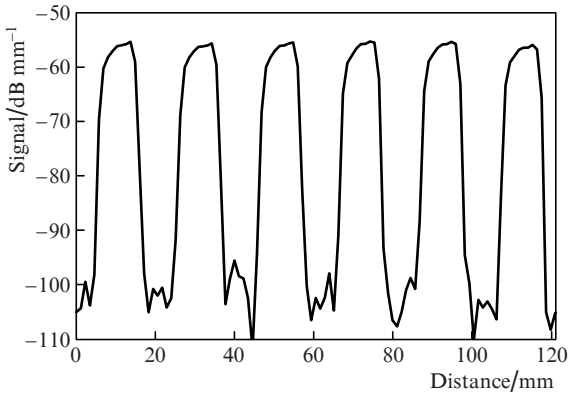

Figure 7. Frequency reflectogram of an FBG array inscribed upon drawing a single-mode from a preform with an erbium-doped germanophosphosilicate glass core.

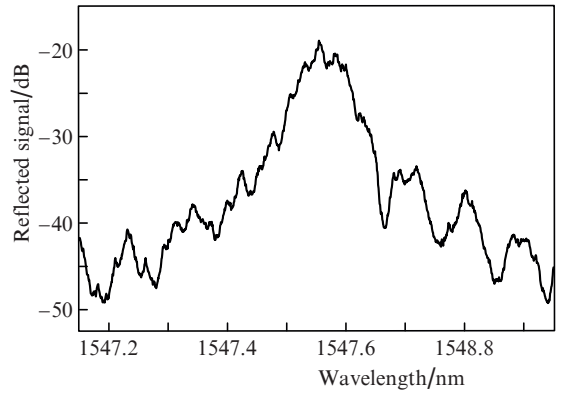

Figure 8. Reflection spectrum of a 1-m-long OF segment with an FBG array inscribed upon drawing an OF from a preform with an erbium-doped germanophosphosilicate glass core.

laser was found to be 6 mW at a pump power of 90 mW; further increase in the pump power does not lead to any changes in the output laser power.

To conclude, we should note again that we investigated the main optical and lasing characteristics of extended FBG arrays fabricated during fibre drawing. A possibility of designing single-frequency fibre lasers based on FBG arrays, including those inscribed in the active-fibre core, is demonstrated.

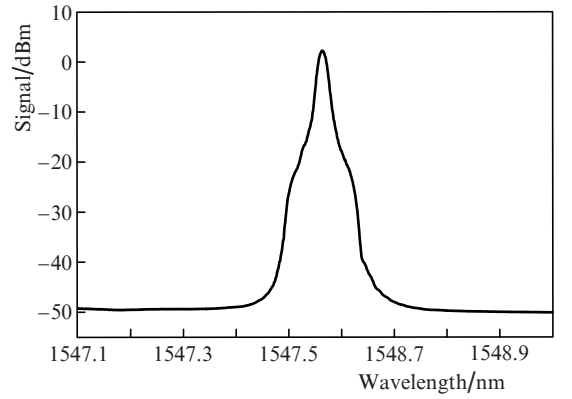

Figure 9. Lasing spectrum of an erbium-doped FBG-array OF, pumped at a wavelength of 1490 nm.

Acknowledgements. This work was performed within a State assignment and supported in part by the Russian Foundation for Basic Research (RFBR) and the National Natural Science Foundation of China (NSFC) (Grant No. 20-57-53013). R.A.A. and L.D.C. acknowledge the support of RFBR (Grant No. 20-08-00822), and F.A.A. acknowledges the support of the Ministry of Education and Science of the Russian Federation (Megagrant No. 2020–220-08–1369) and the Russian Science Foundation (Grant No. 18-12-00457).

References

1. Turitsyn S., Babin S., El-Taher A., Harper P., Churkin D., Kablukov S., Ania-Castañón J., Karalekas V., Podivilov E. *Nat. Photonics*, **4**, 231 (2010).
2. Fotiadi A. *Nat. Photonics*, **4**, 204 (2010).
3. Shatalin S., Treschikov V., Rogers A. *Appl. Opt*., **37**, 5600 (1998).
4. Moore J., Rogge M. *Opt. Express*, **20**, 2967 (2012).
5. Bronnikov K., Wolf A., Yakushin S., Dostovalov A., Egorova O., Zhuravlev S., Semjonov S., Wabnitz S., Babin S. *Opt. Express*, **27**, 38421 (2019).
6. Yatseev V., Zotov A., Butov O. *Results Phys*., **19**, 103485 (2020).
7. Stepanov K., Zhirnov A., Chernutsky A., Koshelev K., Pnev A., Lopunov A., Butov O. *Sensors*, **22**, 6431 (2020).
8. Przhiialkovskii D., Butov O. *Results Phys*., **30**, 104902 (2021).
9. Askins C., Tsai T., Williams G., Putnam M., Bashkansky M., Friebele E. *Opt. Lett*., **17**, 833 (1992).
10. Guo H., Tang J., Li X., Zheng Yu., Yu Hu, Yu Ha. *Chinese Opt. Lett*., **11**, 030602 (2013).
11. Zaitsev I., Butov O., Voloshin V., Vorob'ev I., Vyatkin M., Kolosovskii A., Popov S., Chamorovskii Yu. *J. Comm. Technol. Elec*., **61**, 639 (2016).
12. Popov S., Butov O., Kolosovski A., Voloshin V., Vorob'ev I., Vyatkin M., Fotiadi A., Chamorovski Y. *Proc. PIERS, IEEE Xplore* (St. Petersburg, Russia, 2017) p. 1568.
13. Chamorovskiy Y., Butov O., Kolosovskiy A., Popov S., Voloshin V., Vorob'ev I., Vyatkin M. *Opt. Fiber Technol*., **34**, 30 (2017).
14. Chamorovskiy Yu., Butov O., Kolosovskiy A., Popov S., Voloshin V., Vorob'ev I., Vyatkin M., Odnobludov M. *Opt. Fiber Technol*., **50**, 95 (2019).
15. Popov S.M., Butov O.V., Kolosovskii A.O., Voloshin V.V., Vorob'ev I.L., Isaev V.A., Vyatkin M.Yu., Fotiadi A.A., Chamorovsky Yu.K. *Quantum Electron*., **49** (12), 1127 (2019) [*Kvantovaya Elektron*., **49** (12), 1127 (2019)].
16. Kharasov D.R., Bengal'skii D.M., Vyatkin M.Yu., Nanii O.E., Fomiryakov E.A., Nikitin S.P., Popov S.M., Chamorovsky Yu.K., Treshchikov V.N. *Quantum Electron*., **50** (5), 510 (2020) [*Kvantovaya Elektron*., **50** (5), 510 (2020)].
17. Popov S., Butov O., Bazakutsa A., Vyatkin M., Chamorovskii Yu., Fotiadi A. *Results Phys*., **16**, 102868 (2020).
18. Popov S., Butov O., Bazakutsa A., Vyatkin M., Chamorovskii Yu., Fotiadi A. *Proc. SPIE*, **113571Q** (1 April 2020). DOI: 10.1117/ 12.2557818.
19. https://optosystems.ru/product/cl-5000/.
20. Lipatov D., Guryanov A., Yashkov M., Bubnov M., Likhachev M. *Inorg. Mater*., **54**, 276 (2018).
21. Khudyakov M., Lobanov A., Lipatov D., Abramov A., Vechkanov N., Guryanov A., Melkumov M., Bobkov K., Aleshkina S., Kochergina T., Iskhakova L., Milovich F., Bubnov M., Likhachev M. *Laser Phys. Lett*., **16**, 025105 (2019).
22. Soller B., Gifford D., Wolfe M., Froggatt M. *Opt. Express*, **13**, 666 (2005).
23. Wang Y., Gong J., Wang D., Dong B., Bi W., Wang A. *IEEE Photonics Technol. Lett*., **23**, 70 (2011).
24. Zhang M., Sun Q., Wang Z., Li X., Liu H., Liu D. *Opt. Commun*., **285**, 3082 (2012).

25. Xia Li, Cheng Rui, Li Wei, Liu D. *IEEE Photonics Technol. Lett*., **27**, 323 (2015).
26. Cheng R., Xia Li, Sima C., Ran Ya., Rohollahnejad Ja., Zhou Ji., Wen Yo., Yu Can. *Opt. Express*, **24**, 2466 (2016).
27. Luo Z., Wen H., Guo H., Yang M. *Opt. Express*, **21**, 22799 (2013).
28. Bao X., Chen L. *Sensors*, **11**, 4152 (2011).
29. Schenato L. *Appl. Sci*., **7**, 896 (2017).
30. Hirayama N., Sano Y. *ISA Transact*., **2**, 169 (2000).
31. Butov O., Golant K., Nikolin I. *Electron. Lett*., **11**, 523 (2002).
32. Popov S., Chamorovsky Yu., Mégret P., Zolotovskii I., Fotiadi A. *Proc. ECOC, IEEE Xplore* (Valensia, Spain, 2015) p. 1. DOI: 10.1109/ECOC.2015.7341709.
33. Popov S., Butov O., Chamorovskiy Y., Isaev V., Kolosovskiy A., Voloshin V., Vorob'ev I., Vyatkin M., Mégret P., Odnoblyudov M., Korobko D., Zolotovskii I., Fotiadi A. *Results Phys*., **9**, 625 (2018).
34. Popov S., Butov O., Chamorovski Y., Isaev V., Mégret P., Korobko D., Zolotovskii I., Fotiadi A. *Results Phys*., **9**, 806 (2018).
35. Skvortsov M., Wolf A., Dostovalov A., Egorova O., Semjonov S., Babin S. *J. Lightwave Technol*., **1** (2021). DOI: 10.1109/JLT. 2021.3116758.
36. Rybaltovsky A., Popov S., Lipatov D., Umnikov A., Abramov A., Morozov O., Ryakhovskiy D., Voloshin V., Kolosovskii A., Vorob'ev I., Butov O., Chamorovskiy Yu. *Fibers*, **9**, 53 (2021).